Icosahedral quasicrystal $Al_{71}Pd_{21}Mn_{08}$ and its ξ' approximant: Linear expansivity, specific heat, magnetic susceptibility, electrical resistivity, and elastic constants

C. A. Swenson,* I. R. Fisher,† N. E. Anderson, Jr., and P. C. Canfield
Ames Laboratory, Iowa State University, Ames, Iowa 50011

A. Migliori
Los Alamos National Laboratory, Los Alamos, New Mexico 87545

(Received 4 October 2001; revised manuscript received 18 January 2002; published 8 May 2002)

Linear thermal expansivity (α, 1–300 K), heat capacity (C_p, 1–108 K), magnetic susceptibility (χ, 1–300 K), and electrical resistivity (ρ, 1–300 K) measurements are reported for a single-grain *i*-$Al_{71}Pd_{21}Mn_{08}$ quasicrystal and its $Al_{72}Pd_{25}Mn_{03}$ approximant, and 300 K elastic constants for the quasicrystal. The approximant α (α_{Ap}) and C_p (C_{pAp}) data show ''metallic'' behavior, while the previously reported onset of a transition to a spin-glass state ($T_f < 1.8$ K) dominates α_Q and C_{pQ} below 11 K. C_{pAp} and C_{pQ} superimpose above 16 K when plotted vs T/Θ_0 using the experimental $\Theta_{0Ap} = 455(3)$ K and an adjusted $\Theta_{0ApQ} = 480(4)$ K. The 300 K elastic constants extrapolated to $T=0$ give $\Theta_{0Q}^{el} = 505(1)$ K, suggesting that the normalization is valid only above 16 K. The lattice contribution to C_{pAp} (and, indirectly, C_{pQ}) shows strong (unique) deviations from Debye-like behavior (+3% at 0.84 K for the C_{pAp} data fit). The various Grüneisen parameters (Γ) that are calculated from these data all are positive and normal in magnitude except for a large limiting approximant lattice value, $\Gamma_{0Ap}^{lat} = 11.3$, which may be related to the large dispersion effects in C_p. For the approximant, the combination of anisotropic and large resistivities, a small diamagnetic susceptibility, and a ''large'' linear (electronic) contribution to C_{pAp} ($\gamma_{Ap} = 0.794$ mJ/mol K^2) suggests the existence of a pseudogap in the electronic density of states. The unusually large, highly volume dependent, dispersion at low temperatures for the quasicrystal and its approximant are not consistent with inelastic neutron scattering and other data, and raise questions about the role of phonons in quasicrystals. The present 300 K resistivities can be used with a published correlation to estimate $\gamma_Q \approx 0.25$ mJ/mol K^2.

DOI: 10.1103/PhysRevB.65.184206 PACS number(s): 61.44.Br, 62.20.Dc, 65.40.Ba, 65.40.De

I. INTRODUCTION

Quasicrystals were discovered in the early 1980s in rapidly solidified binary alloys of Al and Mn, Cr, and Fe.[1] Although fine details of the atomic structure are still unresolved, it appears that quasicrystals can possess long-range atomic order but without the usual crystalline requirement of periodicity. The resulting symmetry groups, including face-centered icosahedral as in this case, can show axes of crystallographically forbidden rotational symmetry. Although the first quasicrystalline materials were metastable, reverting to crystalline systems when annealed, several other families of quasicrystals were subsequently discovered, which appear to be thermodynamically stable[2] and which can consequently be synthesized as large single grains via standard crystal-growth techniques.[3] The composition is typically written as for an alloy (in this case $Al_{71}Pd_{21}Mn_{08}$, or Al-Pd-Mn for short), but in most cases one should think of quasicrystals as compounds with a rather well-defined stoichiometry. A major objective of much of the extensive research on quasicrystals is to determine in what manner their physical properties differ from those of normal crystalline or amorphous solids. In one sense, these icosohedral quasicrystals are very similar to amorphous solids, since they are elastically isotropic; their elastic properties are described completely by single longitudinal v_L and (doubly degenerate) transverse v_T sound velocities.[4] In the low-temperature limit, the heat capacities (C_p) of quasicrystals generally have the linear temperature dependence that is characteristic of a metal, although with electrical resistivities which are very much smaller than would be expected, and which, often, have a nonmetallic temperature dependence.[5,6] Optical reflectivity,[7] photoemission, and tunnelling spectroscopy[8,9] studies confirm the interpretation of these results in terms of a pseudogap in the density of states,(DOS) which is centered about the Fermi energy. A paper by Zijlstra and Janssen[10] does not support previous theoretical calculations which have suggested that the electronic DOS at the Fermi level should have a spiky structure, which has not been found experimentally, although the tunnelling results of Escudero *et al.*[8] show a single spiky structure centered in the pseudogap.

The present heat capacity (C_p) and linear thermal expansivity (α) data were obtained using single-grain samples of an *i*-Al-Pd-Mn quasicrystal and its similar, but crystalline, approximant. The following background discussion will be concerned primarily with previous work reported for *i*-Al-Pd-Mn, much of which is complementary to research on other, similar quality, quasicrystals.

Chernikov *et al.*[11] reported C_p (0.06 to 18 K), ac (0.2 to 0.7 K), and static (2 to 300 K) magnetic susceptibility (χ), and magnetization (M) (1.9 to 10 K, to 50 kOe) data for *i*-$Al_{70}Mn_{09}Pd_{21}$. Subsequently, he and his collaborators have reported electrical conductivity and magnetoconductivity,[12] and thermal conductivity[13] results for crystals of this concentration. Lasjaunias *et al.*[14] also have published magnetic and calorimetric results for single grain *i*-$Al_{68.7}Pd_{21.7}Mn_{9.6}$.

Inaba *et al.*[15] give C_p results from 1 to 350 K for a number of quasicrystals, including i-$Al_{70}Pd_{20}Mn_{10}$. Chernikov *et al.*[16] describe C_p (1.5 to 300 K) and thermal conductivity (0.4 to 80 K) results for two *i*-Al-Mn-Pd samples. Wälti *et al.*[17] report C_p results for polygrain i-$Al_{70}Pd_{20}Mn_{10}$ (1.6 to 18 K) and single grain i-$Al_{68.2}Mn_9Pd_{22.8}$ (12 to 300 K) (and *i*-Al-Re-Pd) and conclude that the low-T lattice C_p for Al-Pd-Mn from a previous analysis[11] is appreciably greater than would be expected from sound velocity measurements.[18] After a comparison with calculations from both thermal neutron time of flight[19] and inelastic neutron scattering (INS) (20,21) results, they suggest that the large excess C_p is nonacoustic in origin. Recent coherent inelastic scattering of synchrotron radiation data for *i*-Al-Pd-Mn (Ref. 22) are consistent with the INS results.

Both the C_p and neutron scattering results are related directly to sound velocities. For C_p, the limiting value of the Debye temperature, Θ_0, should correspond to that calculated from $T=0$ sound velocities using Debye theory, and for INS, the initial slopes of the dispersion relations should be equal to the corresponding sound velocities. Amazit and his collaborators used precise sound velocity measurements on i-$Al_{68.7}Mn_{9.6}Pd_{21.7}$ to confirm the elastic isotropy of this material, and to demonstrate that the attenuation is anisotropic.[23] These measurements were extended to 4 K, and a (nonlinear) sound velocity pressure-dependence to 0.3 GPa was measured at 300 K.[18] Further data[24] complement those of Vernier *et al.*[25] to show that tunnelling states exist in these crystals, in agreement with the conclusions from Ref. 13. In addition, these data,[24] although their relative magnitudes are quite normal, have the puzzling features that the pressure dependence of the sound velocities is nonlinear in pressure and is frequency dependent, suggesting relaxation phenomena. Tanaka *et al.*[26] have used the resonant ultrasound (RUS, Ref. 27) technique to determine the (isotropic) sound velocities from 4 to 1073 K of three Al-based icosahedral quasicrystals, including i-$Al_{70}Pd_{24}Mn_6$. They give a tabular comparison of their 290 K elastic constant and other results, and present the temperature dependences graphically. A plot of the ratio of the shear to the bulk modulus for quasicrystals suggests a highly directional bonding which is more similar to that for tetrahedrally bonded solids than for metals. Finally, Amazit *et al.*[28] have used x rays and a diamond cell to determine the compression of powdered i-$Al_{68.7}Mn_{9.6}Pd_{21.7}$ to 40 GPa. The resulting bulk modulus and its pressure dependence are consistent with those from the ultrasonic measurements.[24]

The only thermal-expansion data for Al-Pd-Mn are from x ray lattice parameter (a) determinations over a range of temperature. Yokoyama *et al.*[29] measured $a(T)$ from 300 to 600 K in an investigation of the mechanical properties of i-$Al_{70}Pd_{20}Mn_{10}$. Kupsch and Paufler[30] reported $a(T)$ for i-$Al_{70.3}Pd_{21.7}Mn_{8.0}$ from 15 to 300 K, while the data of Kajiyama *et al.*[31] for i-$Al_{71}Pd_{20}Mn_9$ extended from 10 to 700 K. These three experiments are in essential agreement in overlapping ranges.

The primary objective of the present experiment was to obtain precise linear thermal expansivity (α) data for a bulk single-grain icosohedral quasicrystal for temperatures from 1 to 300 K. The present measurements became feasible when large single-grain samples of i-$Al_{71}Pd_{21}Mn_{08}$, as well as its $Al_{72}Pd_{25}Mn_{03}$ ξ' approximant, became available.[3,32] The low-temperature thermodynamic properties of Al-Pd-Mn quasicrystals, but not the approximant, are complicated below approximately 11 K by the onset of a transition to a spin-glass state, which has been studied in some detail[11,14] and which typically has been described in terms of cluster formation prior to eventual spin freezing ($T_f<1.8$ K). Comparable C_p and α data for these closely related materials allow an estimate to be made of the non-spin-glass contributions to the *i*-Al-Pd-Mn thermodynamics. Other studies[13,25,33] have shown that tunnelling occurs in quasicrystal Al-Pd-Mn at low temperatures. The enhanced α's that often are associated with the onset of tunnelling[34] unfortunately are masked by the onset of the transition to a spin-glass state.

The composition of the Al-Pd-Mn quasicrystalline state is not unique; for this reason, the compositions of the samples have been given for the various experiments that were described above. To avoid inconsistencies in the present measurements, the α and C_p data were taken using a common sample for each material, and the supporting data [electrical resistivity (ρ), susceptibility (χ), and, for the quasicrystal, RUS elastic constants] were from the same material.

II. EXPERIMENTAL DETAILS

Single-grain quasicrystals of *i*-Al-Pd-Mn and single crystals of the closely related ξ' approximant phase were produced by a self-flux technique, as described previously.[3,32] In short, the samples are obtained by slowly cooling the ternary melts of a composition that intersects the primary solidification surface of the desired phase in the equilibrium ternary alloy phase diagram.[35,36] The remaining melt is decanted before crossing any peritectics or eutectic solidification. The technique clearly reveals the growth habit, and results in remarkably large and strain-free samples.[32] The composition of the resulting approximant crystals (via, energy dispersive x ray spectroscopy) is approximately $Al_{72}Pd_{25}Mn_{03}$, with an estimated uncertainty of ± 1 at. %, consistent with the established values. The composition of the icosahedral quasicrystals is $Al_{71}Pd_{21}Mn_8$, as measured by electron microprobe analysis (EMPA), with an estimated error of approximately 0.5 at. % for each element.

Magnetic measurements of the approximant phase were made from 1.8 to 350 K in an applied magnetic field (H) of 10 kOe using a commercial superconducting quantum interference device magnetometer.

Bars for electrical resistivity measurements were cut from well-formed samples using a wire saw (typical bar dimensions were 5 mm long with a 1 mm$\times$1 mm cross section). For the icosahedral phase, the bars had arbitrary orientations with respect to the various high-symmetry directions because the resistivity tensor is believed to be isotropic in an icosahedral symmetry;[37] indeed, no resistivity anisotropies were observed for bars of different orientations. However, bars for the approximant phase were cut either parallel or perpendicular to the pseudofivefold axis [010]. Electrical contact was made to the samples using Epotek H20E, with typical con-

tact resistances of 1–2 Ω. The resistivity was measured using a standard four-probe technique, with a bridge operating at 16 Hz and a current density of approximately $0.1 A/cm^2$. Several samples of each phase were measured to improve confidence in the absolute values of the resistivity.

C_p and α data were taken for a quasicrystal sample and for a ξ' approximant sample; these samples were from the same lots as those used for the magnetization and resistivity measurements. The quasicrystal and approximant samples were irregularly shaped, approximately 11.5(5) mm high, with flat bases (8 mm maximum dimension) and masses of 6.09 g and 3.88 g, respectively. While the shape of the single-grain quasicrystal was similar to that described in Ref. 32, the approximant was roughly pyramidal, with sample growth ocurring in the direction parallel to the [010] axis as rather large (sub-mm cross section) columns that typically fill in to give a dense crystal. The approximant α data were obtained for the sample oriented along [010]; we were unable to produce a suitable sample for measurements in the plane perpendicular to [010]. The formula atomic masses for these two materials are 45.95 g and 47.74 g, respectively. The α data were taken from 1 to 300 K using a differential capacitance dilatometer that was calibrated using high-purity copper.[38] The C_p data were taken from 1 to 108 K using a standard tray-type isothermal calorimeter.[39] The room-temperature elastic constants of an approximately 4 mm^3 sample of this quasicrystal were determined using the RUS technique.[27] The room-temperature density of the RUS quasicrystal, which is needed for the data analysis and was determined from its mass and dimensions ($4.86 g/cm^3$), is consistent with that reported previously ($4.94 g/cm^3$),[32] and is taken to be $4.90(4) g/cm^3$.

III. EXPERIMENTAL RESULTS, DISCUSSION

A. Susceptibility data

We have presented previously the susceptibility of the flux-grown *i*-Al-Pd-Mn phase.[32] Although these data can be characterized by an average magnetic moment of $0.62(2)\ \mu_B$/Mn using our EMPA composition, we note that not all Mn sites are believed to be magnetic in this structure.[14] A better characterization is obtained by comparing the low-temperature (low-T) Curie constant ($C \approx 5 \times 10^{-5}$ emu/g) to that of Lasjaunias and co-workers.[14] In that case, our measured Curie constant can be interpreted as a manganese concentration of 8.5–9.0%,[40] somewhat greater than the value obtained by elemental analysis (8.0%).

The susceptibility of the approximant Al-Pd-Mn phase is shown in Fig. 1. In contrast to the icosahedral phase, the approximant phase is essentially diamagnetic with only a few magnetic impurities. The data shown in Fig. 1 can be represented by the relation $\chi = C/T + AT + \chi_0$, with the parameters $C = 3.218(60) \times 10^{-8}$ emu K/g, $A = -7.4(2) \times 10^{-12}$ emu/g K and $\chi_0 = -9.15(5) \times 10^{-8}$ emu/g; in this relation, the small AT term has no obvious physical significance, and was introduced to improve the Curie-law fit. The very small Curie term (C) corresponds to approximately 1 magnetic Mn out of every 60 000, indicating that this behavior arises from impurity moments. The diamagnetic constant term implies a very low density of states at the Fermi energy.

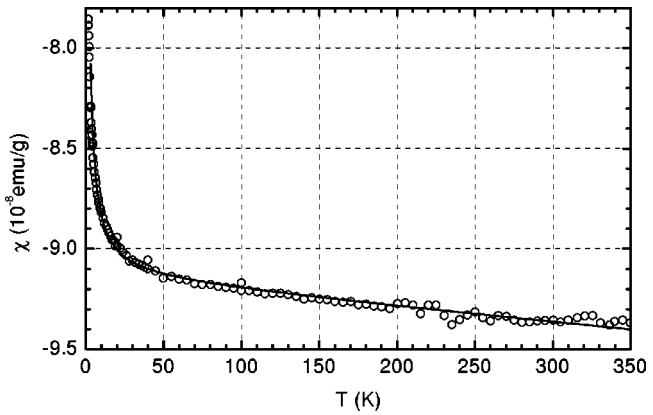

FIG. 1. The susceptibility of ξ' approximant Al-Pd-Mn for an applied field of 10 kOe oriented parallel to [010]. The solid line represents a fit to the data, which is described in the text.

B. Resistivity data

The temperature dependences of the electrical resistivities (ρ) of the icosahedral and the ξ' phases are shown in Fig. 2. The resistivity of the icosahedral phase [Fig. 2(a)] is typical of many quasicrystalline systems, being at least superficially similar to that of a disordered alloy,[41] with the pronounced

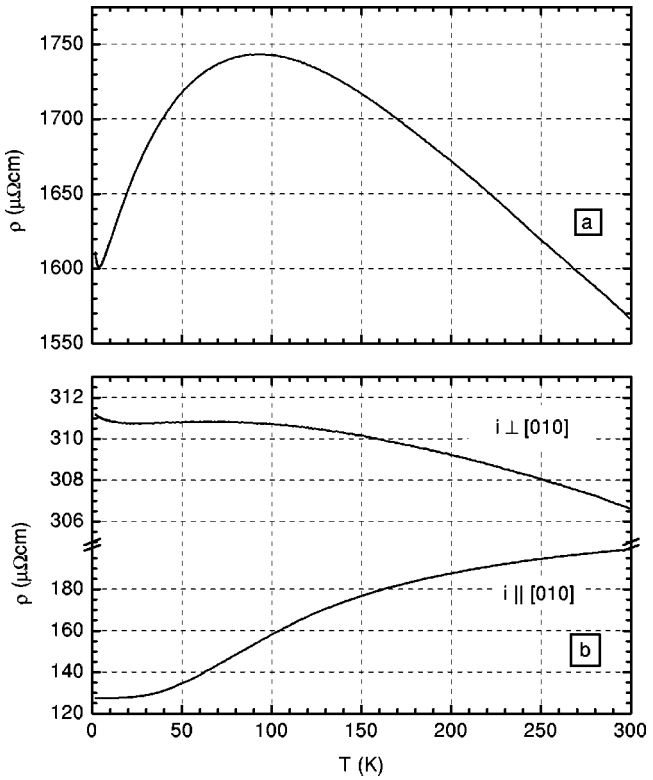

FIG. 2. The resistivities of (a) icosahedral Al-Pd-Mn and (b) approximant Al-Pd-Mn as a function of temperature. The sample orientation is arbitrary for the icosahedral phase, but is as noted for the approximant phase (note the split resistivity scale for the different orientations).

maximum in the resistivity due to weak localization with strong spin-orbit scattering.[42] The resistivity of the approximant phase [Fig. 2(b)] is somewhat lower than that of the icosahedral phase, and shows a much weaker temperature-dependence, which, however, still is characterized by the effects of weak localization. While the resistivity for currents (*i*) flowing perpendicular to the *b*-axis ($i\perp[010]$) was reasonably reproducible from sample to sample, that for $i\|$ [010] showed a rather large variation. The ξ' structure may be extremely susceptible to defects introduced in the cutting and polishing process that was used to prepare the resistivity bars;[43] this certainly is not the case for the icosahedral phase. Despite the sample-to-sample variation, the resistivity for currents flowing in the pseudofivefold direction [010] is consistently lower than that for currents flowing in the perpendicular direction, reminiscent of the behavior of the electrical conductivity of decagonal Al-Ni-Co.[44,45] However, in the case of decagonal Al-Ni-Co, the resistivity is that of a moderately good metal for currents flowing in the crystalline direction (along the ten-fold axis), whereas the present data indicate that weak localization is significant to a greater or lesser extent for all current orientations in ξ' Al-Pd-Mn.

Below approximately 4 K, the resistivities of both materials show a slight upturn, with the temperature dependences of the corresponding conductivities ($\sigma=1/\rho$) (not shown) qualitatively consistent with the relation given by Chernikov *et al.*,[12]

$$\sigma=\sigma_0+aT^{0.5}. \tag{1}$$

C. RUS elastic constants

A RUS measurement[27] determined the room-temperature sound velocities (elastic constants) of a 4 mm cube of the same *i*-$Al_{71}Pd_{21}Mn_{08}$ quasicrystal material that was used for the C_p and α measurements. While time-of-flight velocity measurements determine velocities along symmetry directions, an RUS determination utilizes fits of the resonance frequencies to an elastic model for a large number of propagation directions in the sample (in this instance, 42), and thus gives direct information that is not available in other sound velocity measurements,[46] or in neutron-scattering experiments. The current results are consistent with the assumption of elastic isotropy,[4,23,46] with only two parameters required to fit the results. The parameters (calculated using the density $\varrho=4.86$ g/cm^3) are $C_{11}=C_{22}=C_{33}=2.134(10)\times10^{11}$ Pa, $C_{44}=C_{55}=C_{66}=0.6891(14)\times10^{11}$ Pa, and $C_{12}=C_{13}=C_{23}=(C_{11}-2C_{44})=0.756(3)\times10^{11}$ Pa. The major uncertainty in these measurements is in the value of the longitudinal modulus, C_{11}, 0.5%; the uncertainty in C_{44} is 0.2%. The resulting room-temperature adiabatic bulk modulus is $B_S=(1/3)(C_{11}+2C_{12})=[C_{11}-(4/3)C_{44}]=1.215(10)\times10^{11}$ Pa, with the isothermal bulk modulus, $B_T=1.189(10)\times10^{11}$ Pa.[47] For the present purposes, these elastic constant (sound velocity) data are important for calculating the limiting, $T=0$, value of the characteristic Debye temperature, Θ_0.[48,49] Θ_0 is calculated from an average 0 K sound velocity as[50]

$$\Theta_0^3=[(h/k_B)^3(3rN_0/4\pi V_m)(1/\langle 1/v^3\rangle)] \tag{2a}$$

and for an isotropic quasicrystal (two sound velocities; v_L and a twofold degenerate v_T)

$$=\{(h/k_B)^3(3rN_0/4\pi V_m)v_T^3\{3/[2+(v_T/v_L)^3]\}\} \tag{2b}$$

$$=\{(2.5142\times10^{-3})^3(r/V_m)v_T^3\{3/[2+(v_T/v_L)^3]\}\}, \tag{2c}$$

where h is the Planck's constant, k_B the Boltzmann constant, N_0 the Avogadro's number (per g mol), V_m the molar volume (m^3/g mol), r the number of atoms/unit cell, and the sound velocities are in m/s. These velocities are related to the elastic constants as $C_T=C_{44}=\varrho v_T^2$, and $C_L=C_{11}=\varrho v_L^2$. Note that the density ϱ enters into Eqs. (2) only through the definition of the molar volume.

The present sound velocity (elastic constant) data are for room temperature. Since the *i*-Al-Pd-Mn sound velocities (elastic constants) have only a small (negative) temperature-dependence,[18] $\Theta_0=498(1)$ K as calculated for 300 K corresponds to a minimum $T=0$ value; the uncertainty in Θ_0 results primarily from the uncertainty in v_T (or C_{44}). The relative volume change from 0 to 300 K [+0.72%, from $\alpha(T)$] and the magnitude of the Grüneisen parameter (1.88) can be used (see below) to estimate the $T=0$ value, $\Theta_{0Q}=505(1)$ K, which will be compared with calorimetric results in the following section. No RUS data were obtained for the approximant because of the difficulty in obtaining a completely dense cube of the required dimensions.

Table I gives a summary for *i*-Al-Pd-Mn of Θ_0's that have been calculated from published longitudinal and transverse sound velocities using Eqs. (2). Amazit and his collaborators[18,23,24] used large single-grain samples and obtained velocity measurements from 300 to 4 K, while the RUS data of Tanaka *et al.*[26] were for 4 to 1073 K. These RUS Θ_0 results are estimated to have a systematic uncertainty of less than 1.5% due to second phase effects, and a precision of better than 0.5%. The differences in the values of the room temperature Θ_0's (including the present data) are appreciably larger than can be implied from their precision, and, qualitatively, vary inversely with the Mn concentration. The correlation with atomic mass is less pronounced.

While an average value probably is not appropriate, the magnitudes of Θ_0 at 300 K and 0 K are 492(11) K and 504(10) K, respectively. This conclusion will be important for discussing large dispersion effects in C_p for the present samples. A puzzle is that $\Delta\Theta_0=\Theta_0(0\text{ K})-\Theta_0(300\text{ K})$ is significantly larger for the directly measured experimental data [+12(2) K] than the one that follows from the relative volume change and the (temperature independent) Grüneisen parameter [7(1) K].

D. Representation of α and C_p data

Low-temperature α and C_p data for most solids can be represented by power series that contain only odd powers of T,[48,49]

TABLE I. A summary of C_p-related parameters from various references and from the present experiments. Figures 6 suggest that the spin-glass contributions to *i*-Al-Pd-Mn become important for $T < 11(1)$ K$[T/\Theta_0 < 0.022(2)]$. See the text for details.

Θ_0	γ	Sample	Comments
(K)	(mJ/mol K^2)		
455(3)	0.749(1)	$Al_{72}Pd_{25}Mn_{03}$	C_p, present, ξ', approximant
362(6)	0.40(12)	*i*-$Al_{70}Pd_{21}Mn_9$	C_p, Ref. 11
480(1)		*i*-$Al_{68.7}Pd_{21.7}Mn_{9.6}$	US, 300 K (Refs. 18,23,24)
493(1)		*i*-$Al_{68.7}Pd_{21.7}Mn_{9.6}$	US, 4 K (Refs. 18,23,24)
503(3)		*i*-$Al_{70}Pd_{24}Mn_6$	RUS, 290 K (Ref. 26)
514(3)		*i*-$Al_{70}Pd_{24}Mn_6$	RUS, 4 K (Ref. 26)
498(1)		*i*-$Al_{71}Pd_{21}Mn_{08}$	RUS, 300 K, Present
505(1)		*i*-$Al_{71}Pd_{21}Mn_{08}$	RUS, $T=0$, via Γ_Q^{lat}
480(4)	<0.4	*i*-$Al_{71}Pd_{21}Mn_{08}$	From C_{pApQ}
	0.25(10)	*i*-$Al_{71}Pd_{21}Mn_{08}$	Mizutani(Ref. 5)

$$\alpha/T = \sum_{n=0}^{N} A_{2n+1} T^{2n}, \tag{3a}$$

$$C_p/T = \sum_{n=0}^{N} C_{2n+1} T^{2n}. \tag{3b}$$

The lead parameters, A_1 and C_1, generally are ascribed to electronic contributions, with $C_1 = \gamma$, the electronic specific-heat coefficient, although, for amorphous solids, a linear term also has been associated with a distribution of tunnelling states.[34] In most instances, higher-order terms are associated with lattice properties (C_p^{lat}), with Θ_0 [Eqs. (2)] given by[50]

$$\Theta_0^3 = [(12\pi^4/5) rR/C_3]$$

$$= [1.944 \times 10^6\, r(\text{mJ/g mol K})/C_3]\,\text{K}^3, \tag{4}$$

where R is the gas constant. Equation (4) has no significance for tunneling systems, where the''lattice'' contribution C_3 often is appreciably greater than would be calculated from Eqs. (2).[34]

The form of Eq. (3b) follows from the requirement that the lattice DOS have the same values for positive and negative energies,[51] and should be valid over an appreciable temperature range upwards from 0 K. Equation (3b) often is fit to experimental data using only the first two or three terms. This is reasonable if the available temperature range and precision of the data are limited. The extension of the fits to include higher-temperature data (if available) and the use of higher-order terms can result in a (slight) increase in C_1 $(=\gamma)$ and a significant decrease (increase) in C_3 (Θ_0). A continuity in the slope between the low-temperature fit and the higher-temperature data is very important.

For a metal with only electronic and lattice contributions, C_1 and C_3 should remain unchanged for a series of fits of Eq. (3b) to the data that have a common initial temperature and increasing maximum values of T (and number of terms, determined by the precision of the data). How important are the higher-order terms, or, equivalently, deviations from Debye-type behavior (dispersion effects), at low temperature? For the lattice contribution, C_p^{lat} [$n>1$ in Eq. (3b)], a 3% deviation from a constant C_p^{lat}/T^3 occurs near $\Theta_0/10$ for the Debye function,[50] 10.3 K for copper (Ref. 39, $\Theta_0 = 345$ K), 3.7 K for GaAs (Ref. 52, $\Theta_0 = 345$ K), 1.5 K for zinc metal (Ref. 52, $\Theta_0 = 327$ K), and 0.84 K for the present approximant ($\Theta_0 = 455$ K, see the following section). The fits of Eq. (3b) to the C_p data for the ξ' approximant require five parameters for 1.38 to 10 K, seven for 1.38 to 20 K, and ten for 1.38 to 30 K. The resulting C_1 and C_3 values are internally consistent, and correspond to $\gamma = 0.794(1)$ mJ/mol K^2 and $\Theta_{0Ap} = 455(3)$ K.

One consequence of the above discussion is that the dispersion effects are difficult to predict in advance for the low-temperature C_p data, so Eq. (3b) cannot be used reliably to fit a limited range of ''high-T'' data to obtain magnitudes for C_1 and C_3. The number of terms and the accuracy of the data required for such an extrapolation probably are unrealistic in practice.

Equations (3) suggest that at low temperatures, $\alpha(T)$ $[C_p(T)]$ be plotted as α/T (C_p/T) vs T^2 to obtain A_1 (C_1) and A_3 (C_3) from the intercept and limiting slope. This representation becomes unwieldy as C_p increases rapidly with increasing temperature (even for a Debye solid), so, more conveniently, the predominantly lattice C_v's $[C_v^{lat} = C_v(T) - \gamma T]$ are represented as equivalent Debye Θ's.[49] For a C_v^{lat} datum at T, $\Theta(T)$ is the Debye temperature which, when used in the Debye relation for C_v (C_{Debye}, Ref. 50), will give the same C_v at that temperature,

$$C_v^{lat}(T) = C_v(T) - \gamma T = C_{Debye}[\Theta(T)/T]. \tag{5}$$

A plot of $\Theta(T)$ vs T then represents deviations of the data from the Debye function, or the effects of dispersion; a decreasing Θ represents an increasing positive deviation of C_v from Debye behavior. For most solids (including those discussed in a preceding paragraph), $\Theta(T)$ initially is a constant (Θ_0), then, as dispersion becomes important, decreases with increasing temperature to a minimum (near $\Theta_0/10$ for fcc and bcc solids), and approaches a constant value (Θ_∞) at

higher temperatures. The discussion of C_p results in Sec. III E includes examples of this behavior. If C_p is used in Eq. (5) rather than C_v, $\Theta(T)$ will decrease with increasing T at "high" T since $C_v < C_p$.[47] Inaba *et al.*[15] have presented their C_p (corrected to C_v) data using equivalent Θ's. A similar, usually smaller, effect occurs because Θ also will decrease as the sample expands with increasing T.

In the quasiharmonic approximation,[48,49] the lattice C_v's of similar solids should overlap when plotted vs T/Θ_0; that is, $C_v^{lat}(T/\Theta_0)$ for related solids. This is strictly true for Debye solids, but also, qualitatively, for more sophisticated lattice dynamics models. Because of the strong temperature dependence of C_v for $T < \Theta_0$, comparisons of $C_v^{lat}(T/\Theta_0)$ for different solids are made most easily and sensitively through plots of Θ/Θ_0 vs T/Θ_0, where Θ is the equivalent Debye temperature [Eq. (5)], and Θ_0 is obtained from fits of Eq. (3b) to the data, or from Eqs. (2).

The representation of α data using Eq. (3a) is strictly for convenience, although the separation into electronic and other contributions is valid. As the following discussion will show, the lattice contribution to α involves not only C_p, but also its temperature-dependent volume dependence through the Grüneisen parameter. Hence, Eq. (3a) does not have the same fundamental basis as Eq. (3b), and fits of it to α data for various temperature ranges are not as consistent as those of Eq. (3b) to C_p.

In the quasiharmonic model,[48,49] the volume thermal expansivity ($\beta = 3\alpha$ for an isotropic solid) is proportional to C_v/V (C_p/V), with the proportionality factor involving the isothermal bulk modulus B_T (adiabatic bulk modulus, B_S) and the dimensionless Grüneisen parameter, Γ,

$$\beta = 3\alpha = \Gamma(C_v/B_T V) = \Gamma(C_p/B_S V). \tag{6a}$$

since $C_p/C_v = B_S/B_T$.[47] If independent (separable) contributions (electronic, lattice, magnetic, etc.) to the thermodynamics of an isotropic solid can be identified, each contribution will have a C_{vi} and a Γ_i associated with it, and the individual thermal expansivities will be additive to give

$$\beta = \sum \beta_i = 3\sum \alpha_i = \sum \Gamma_i C_{vi}/B_T V. \tag{6b}$$

In this model, the Γ_i are functions of the volume dependence of the characteristic energy, Φ_i, which is associated with the contribution (Θ_0 for the lattice, the Fermi Energy for free electrons, the Curie temperature for a magnetic system, etc.), with

$$\Gamma_i = 3\alpha_i B_T V/C_{vi} = -d\ln\Phi_i/d\ln V. \tag{7}$$

While values of Γ typically range from ± 1 to ± 4 (Ref. 48), Γ will have much larger magnitudes when Φ has a large volume sensitivity, such as that associated with tunneling.[34,48] The lattice Γ_i, Γ^{lat}, generally has a temperature dependence similar to that of $\Theta(T)$, since the lattice modes that are excited with increasing T may have significantly different volume-dependences. By analogy with $\Theta(T)$, Γ_0^{lat} is the limiting, $T=0$ value of $\Gamma^{lat}(T)$, and, at high T, Γ^{lat} approaches a limiting constant value, Γ_∞^{lat}. Since $\Gamma_0^{lat} = -d\ln\Theta_0/d\ln V$, Θ_0^{lat} also can be calculated from the volume (pressure) dependence of the sound velocities [Eqs. (2)].

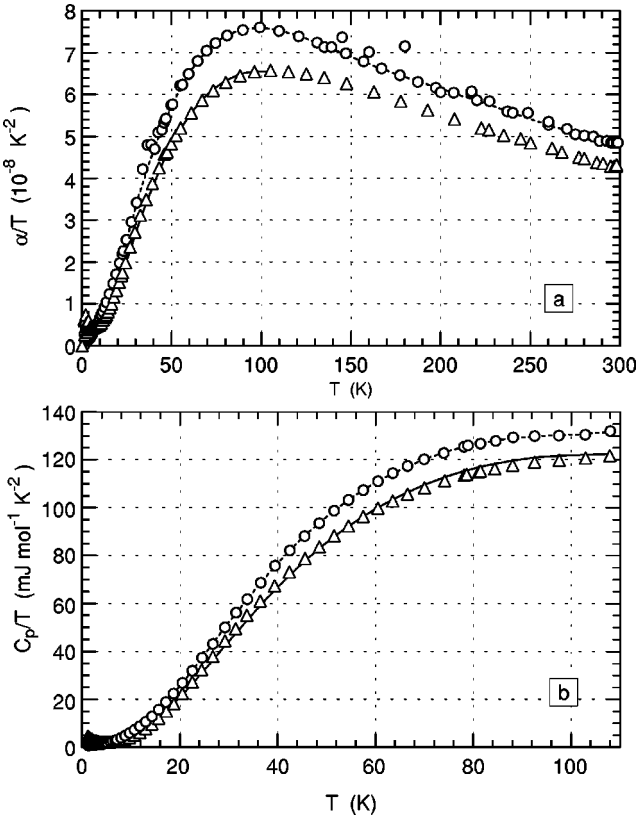

FIG. 3. α/T and C_p/T vs T for the Al-Pd-Mn data. In Figs. 3–5, (○) and (△) are the approximant and quasicrystal data, (- - -) and (- - -) are the smooth representations of these data, (—) is a normalization of the approximant data to those for the quasicrystal for $T > 16$ K, and an extrapolation for $T < 16$ K.

The results of the RUS experiment [$B_T = 1.189(10) \times 10^{11}$ Pa, $V_m = (\text{molecular weight})/\varrho = 9.40 \times 10^{-6}$ m^3/g mol] give $(3B_T V)_Q = 3.35 \times 10^9$ mJ/g mol for the quasicrystal at room temperature. Similar data do not exist for the approximant, but a general discussion of the equations of state of solids[53] suggests that, to a first approximation, the product $B_T V$ is a characteristic energy that should be the same for similar solids. In the following, we will assume that $(3B_T V)_{Ap} = (3B_T V)_Q$, independent of T.

E. α and C_p data

The actual α and C_p data shown as a function of T in Figs. 3 and 4 have been normalized by T to compensate partially for the rapid temperature dependence. Above 140 K, the approximant α's (α_{Ap}) showed long time constants and scatter, which most likely are associated with the sample inhomogeneities; the quasicrystal α's (α_Q) were much more consistent. While the approximant data (○) are systematically greater than those for the quasicrystal (△) down to 11 K, the slopes of both α_Q/T and C_{pQ}/T begin to decrease rapidly on cooling below this temperature (Figs. 4), indicating the onset of the transition to a spin-glass state. The solid

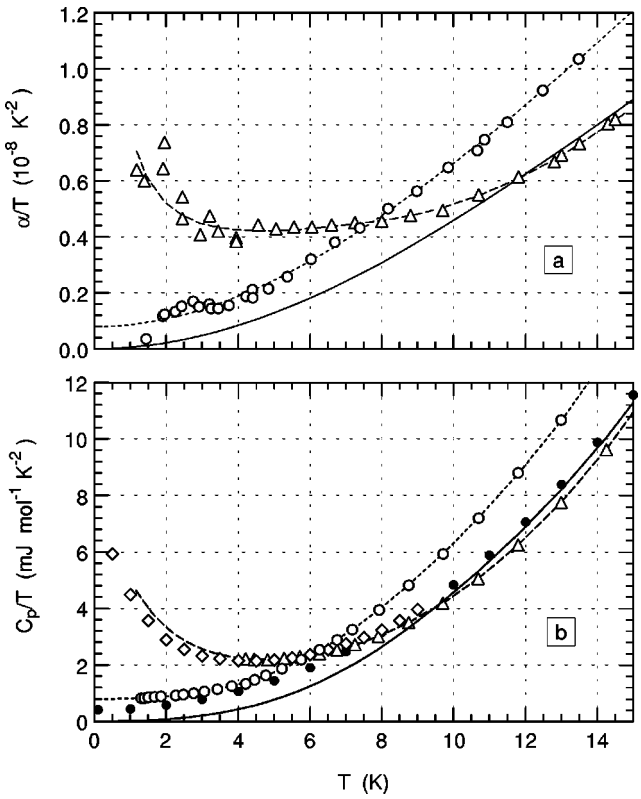

FIG. 4. See Figs. 3. In addition, (●) are a smooth representation of the 8–18 K data and its extrapolation to 0 K from Ref. 11, with (◇) the actual data for $T<9$ K.

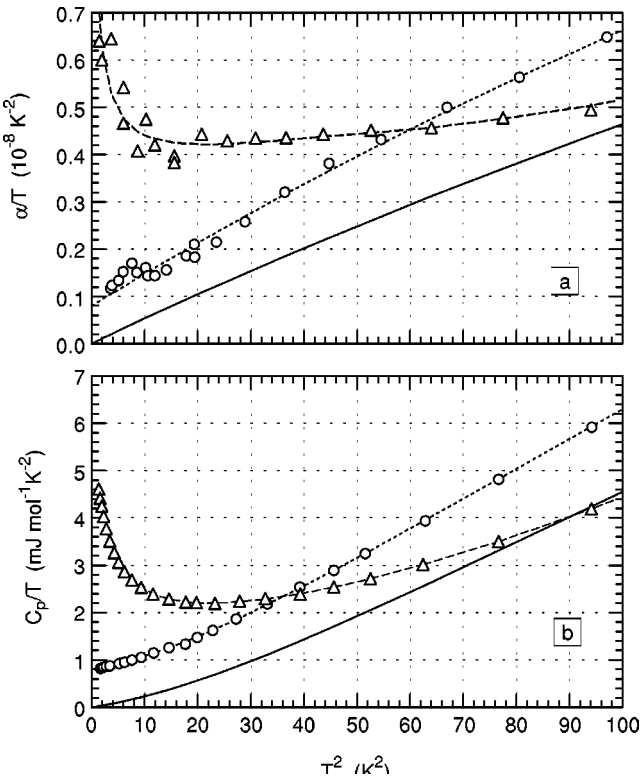

FIG. 5. α/T and C_p/T vs T^2 for the Al-Pd-Mn data; the symbols and smooth relations are as in Figs. 3.

curves in Figs. 3–5 (—) represent approximant-based extrapolations of the higher temperature α_Q and C_{pQ} data to $T=0$ (α_{ApQ},C_{pApQ}, see below). Figure 4(b) also shows the smooth fit to the 8 to 18 K quasicrystal C_p data from Ref. 11 (●) and its extrapolation to $T=0$ (Table I), as well as the actual data (◇) for $T<9$ K. The overall agreement between the present C_{pQ} data (△) and those from Ref. 11 is satisfactory. The C_p's from 1 to 7 K as given in Ref. 14 are significantly larger than these, for reasons that are not understood, but which may be related to a greater Mn content.[40] The C_p data of Inaba *et al.*[15] are somewhat smaller than the present C_p's for $T<30$ K, but are in essential agreement from 80 to 108 K. Again, their sample composition is somewhat different from ours. Wälti *et al.*[17] report that C_p data for polygrain $Al_{70}Mn_9Pd_{21}$ (1.6 to 18 K, Ref. 11) and single-grain $Al_{68.2}Mn_9Pd_{22.8}$ (12 to 300 K) samples coincide in the overlap region, which suggests that differences in Al and Pd content are not significant above 12 K. These data also are consistent with the present data to 108 K.

The present α_Q results can be compared with the temperature-dependences of (isotropic) x ray lattice parameters given by Yokoyama *et al.*[29] (300 to 600 K for i-$Al_{70}Pd_{20}Mn_{10}$), Kupsch and Paufler[30] (15 to 300 K for i-$Al_{70.3}Pd_{21.7}Mn_{8.0}$) and Kajiyama *et al.*[31] (10 to 700 K for i-$Al_{71}Pd_{20}Mn_9$). The relative lattice parameter changes from 0 to 300 K for the latter two determinations are in excellent agreement with the corresponding relative length change from the present data, 2.39×10^{-3}. The 300 K α's reported for these x ray data are, respectively, 1.3×10^{-5}/K (300 to 600 K), 1.44×10^{-5}/K, and $1.316(8)\times10^{-5}$/K (180 to 600 K average), to be compared with the present $1.29(1)\times10^{-5}$/K. Unfortunately, no comparable x ray data exist for the approximant, where α possibly (most likely) is anisotropic.

Equations (3) suggest the α/T (C_p/T) vs T^2 plots of Figs. 5, where the low-temperature α data show more scatter than those for the higher precision C_p's. The scatter in α_{Ap} below 4 K (approximately $\pm10^{-9}$/K) is normal, but that for α_Q is excessive. The smooth representations through the data points in Figs. 3–5 [(- - -) for α_{Ap}, C_{pAp}; (– – –) for α_Q, C_{pQ}] were generated from power series fits to the data.[54]

While the low-temperature α_Q and C_{pQ} data in Figs. 5 are inconsistent with Eqs. (3) because of the spin-glass transition, both the α_{Ap}, and C_{pAp} data can be represented by Eqs. (3). Although it is not evident in Figs. 3–5, a close correspondence between the shapes of the approximant and quasicrystal $C_p(T)$ above 15 K can be used to approximate the lower temperature, non-spin-glass $C_p(T)$ for the quasicrystal. This shape similarity is evident in the equivalent $\Theta(T)$ [Eq. (5)] plots of Fig. 6(a), where $\Theta_{Ap}(T)$ (○) was calculated from C_{pAp}^{lat}, and $\Theta_Q(T)$ was calculated using total C_{pQ} data (△), since the spin-glass transition masks contributions linear in T. The rapid decrease in Θ_Q on cooling below 11 K reflects the excess (spin glass) C_{pQ} in Figs. 4(b) and 5(b) (smaller Θ's represent larger C_p's). The closed circles (●) below 20 K are Θ's (Θ_{Ap}^{tot}) for the total C_{pAp} data [$\gamma_{Ap}=0$ in Eq. (5)]. If γ_Q were comparable to γ_{Ap}, $\Theta_Q(T)$ would resemble Θ_{Ap}^{tot} between 10 and 20 K. Equivalent Θ calculations

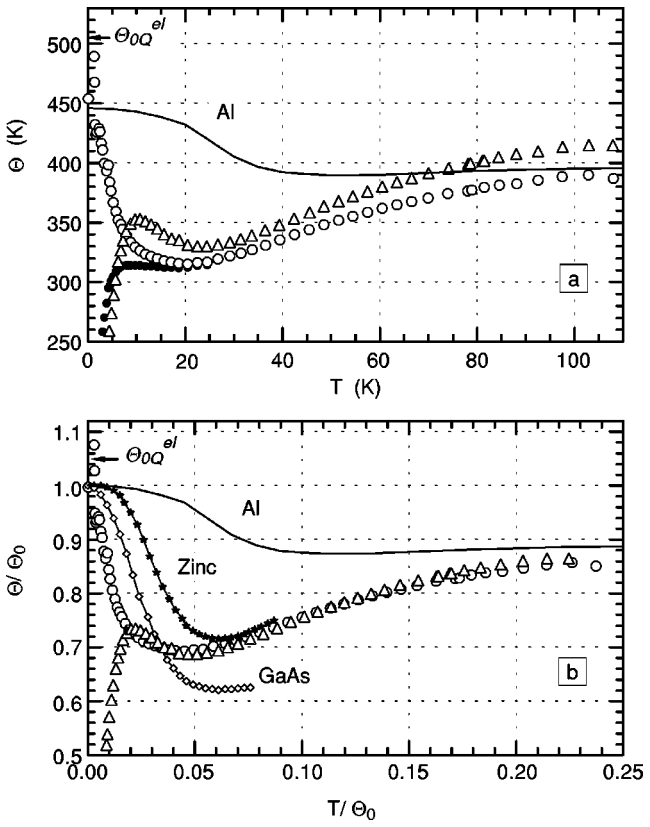

FIG. 6. Temperature dependence of equivalent Debye Θ's [Eq. (5)]; (○) approximant lattice, (△) quasicrystal data, (●) total approximant data, (—) metallic aluminum. In (b), $\Theta_0=455$ K for the approximant and 480 K for the quasicrystal; smooth values also are shown for GaAs (⋆) and metallic zinc (◇). The RUS value, $\Theta_{0Q}^{el}=505(1)$ K, also is indicated. See the text for details.

using the form of C_{pAp} with varying γ's suggest that $\gamma_Q > 0.4$ mJ/mol K^2 probably would affect the shape of $\Theta_Q(T)$ in Figs. 6. The result of the RUS experiment, $\Theta_{0Q}^{el}=505(1)$ K, also is shown in Fig. 6(a). Since the major component in these materials is aluminum, equivalent Θ's for the lattice C_p of this metal are included in Fig. 6(a). The dimensionless (Θ/Θ_0 vs T/Θ_0) plot of Fig. 6(b) provides a quantitative test of the apparent similarity above 20 K in Fig. 6(a). The choices of $\Theta_{0Ap}=455$ K (as above) and $\Theta_{0ApQ}=480(1)$ K [in absolute terms, 480(4) K] give a close correspondence between the two sets of data above approximately 16 K. The normalized C_p's (C_{pApQ}), shown as (—) in Figs. 3(b)–5(b), were calculated by replacing T in the power-series representations for C_{pAp} by $T\times(455/480)$. C_{pApQ} reproduces C_{pQ} from 16 to 108 K with a standard deviation of 2%; the extrema are ±3%, and are systematic. On cooling below 16 K ($T/\Theta_0=0.033$), C_{pQ} is slightly smaller than C_{pApQ} (Θ larger), with the C_p difference changing sign and increasing rapidly (Θ_Q decreasing) below 11 K ($T/\Theta_0<0.02$); see Figs. 4(b)–6(b). This onset of the spin-glass transition on cooling occurs at a higher temperature (11 K) than has been assumed previously,[11,14] but could be a function of the composition of the sample.

The $T=0$ RUS result, $\Theta_{0Q}^{el}=505(1)$ K, is 5% larger than $\Theta_{0ApQ}=480(4)$ K from the normalization to the approximant data; this is consistent with the implication from Fig. 6(b) that the normalization slightly overestimates C_{pAQ} ($\Theta_{ApQ}<\Theta_Q$) between 11 and 16 K. The relative agreement between these two determinations of Θ_{0Q} (and other results; see Table I) provides (an indirect) assurance that the fitting of Eq. (3b) to the C_{pAp} data and the extrapolation of this fit to $T=0$ are reasonable. Unfortunately, we were unable to obtain sound velocity data for the approximant.

The rapidity of the decrease in Θ_{Ap} with increasing temperature in Figs. 6, which is a measure of dispersion or non-Debye behavior, is very unusual. For comparison, the reduced Θ's for three typical materials, two of which have large dispersion, also are plotted in Fig. 6(b). These are a typical cubic metal (Al, $\Theta_0=447$ K, as in Ref. 55; see also Ref. 56), the tetrahedrally bonded semiconductor GaAs ($\Theta_0=345$ K, Ref. 52), and the anisotropic zinc metal ($\Theta_0=327$ K, Ref. 52) [see the discussion following Eqs. (3) and (4)]. A primary conclusion from Fig. 6(b) is that the approximant, and, presumably, also the quasicrystal, show greater dispersion effects on warming than has been reported previously for any material.

Various dimensionless Grüneisen parameters, Γ [Eq. (7)], are plotted as a function of T/Θ_0 in Figs. 7, and are summarized in Table II, where correlations with other data are given. The extent of the *y*-axis in Fig. 7(a) corresponds to the maximum temperature (nominally 108 K) for the C_p data. The data points were calculated from Eq. (7) using the actual α data and C_p's calculated from the appropriate smooth relation. Γ_Q (△) and Γ_{Ap}^{tot} (●) are calculated from the total α and C_p data for each, and Γ_{Ap}^{lat} (○) from the approximant lattice contributions. The upper Γ_{Ap}^{lat} curve (– – –) is calculated using the smooth lattice relations, with an extrapolated $T=0$ value, $\Gamma_{0Ap}^{lat}=11.3$.

These plots reflect sensitively the experimental scatter in $\alpha(T)$; note the "bump" in Γ_{Ap}^{lat} at 0.08 in Fig. 7(a), which is barely apparent at 35 K in Fig. 3(a), and the scatter of the Γ's below 0.01 in Fig. 7(b). The small magnitudes of α_{Ap}^{lat} and C_{pAp}^{lat} for $T/\Theta_0<0.008$ (<3.8 K, Figs. 5) give meaningless values of Γ_{Ap}^{lat} for the α data, and only the smooth (extrapolated) Γ_{Ap}^{lat} is relevant. The lower (– – –) curve, Γ_{Ap}^{tot}, was calculated from the total α_{Ap} and C_{pAp} relations. While the linear terms in the fits to α_{Ap} and C_{pAp} give $\Gamma_{0Ap}^{tot}=\Gamma_{lin}=3.38$, a more reasonable graphical average through the data [Fig. 7(b)] gives $\Gamma_{lin}=4.1(5)$. The fits to α_Q and C_{pQ} give the smooth Γ_Q relation (- - -) that has a maximum at 0.01 (5 K). Because of the spin-glass transition,[11,14] Γ_Q cannot be extrapolated below the present data (roughly 1 K, or $T/\Theta_0\approx0.002$). Since the quasicrystal lattice contributions to α_Q and C_{pQ} are very small below 3 K (Figs. 4 and 5), the low-temperature Γ_Q should be that of the spin-glass state; a graphical average gives $\Gamma_{spin\ glass}=6(1)$. The Γ's for the two solids in Fig. 7(a) are parallel from approximately 14 to 108 K ($T/\Theta_0\geqslant0.03$), with $\Gamma_{ApQ}=0.948\,\Gamma_{Ap}^{lat}$ [(—) in Figs. 7] reproducing Γ_Q from 14 to 108 K with a standard deviation of 0.8% and maximum differences of ±1.5%. The corresponding extrapolated $\Gamma_{0ApQ}^{lat}=10.7$ probably is too small because of the systematic differences between Γ_{ApQ} and Γ_Q

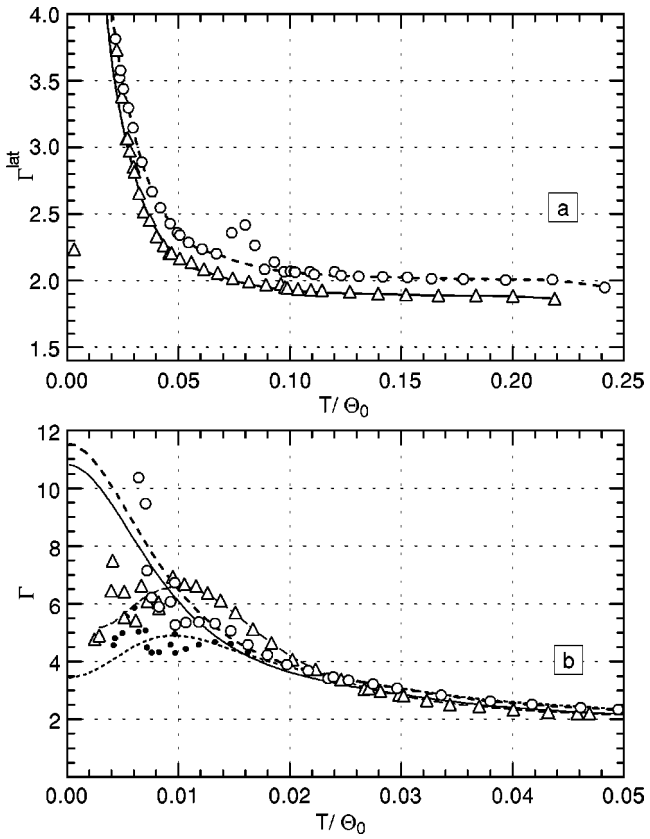

FIG. 7. Grüneisen parameters (Γ) for the Al-Pd-Mn data. The symbols are as in Figs. 6, with (—) smooth representations of Γ_{Ap} (both lattice only and total), and (—) a smooth representation of Γ_Q. (—) is a smooth normalization, Γ_{ApQ}, of Γ_Q to Γ_{Ap}. See the text for details.

from 0.025 to 0.012 in Fig. 7(b). The small incertainty in the values of $B_T V$ that are used [Eq. (7)] does not affect qualitatively the scaling between Γ_Q and Γ_{Ap}.

An extension of Γ_Q from 108 to 300 K using C_p's from Inaba *et al.*[15] (not shown) gives $\Gamma_Q = 1.88(2)$, independent of T, in good agreement with Fig. 7(a) (Table II). Kajiyama *et al.*[31] have combined their *i*-Al-Pd-Mn x ray expansivities with C_p data from Inaba *et al.*[15] and the elastic constants of Tanaka *et al.*[26] to calculate Γ's from 20 to 350 K, which are approximately temperature independent, and are in agreement with those in Fig. 7(a) (Table II). The difference between our 300 K RUS value of Θ_0 (498 K) and its value at 0 K was estimated using Eq. (7) with the volume change from the α_Q data, $d\ln V = -7.2\times10^{-3}$ and a constant $\Gamma = 1.88$, giving $d\ln\Theta_0 = 0.0135$, or, $\Delta\Theta = +7$ K, and $\Theta_0(0\text{ K}) = 505$ K.

TABLE II. Values for the limiting Grüneisen parameters [Γ, Eq. (7)], which follow from the present α and C_p data for *i*-Al-Pd-Mn (Quasi) and its ξ' approximant (Ap), and other determinations. See the text for details.

Γ	Quasi	Ap	Comments
Γ_0^{lat}	10.7	11.3	Fig. 7(b).
Γ_∞	1.88(3)	1.98(2)	Present, 100 K, Fig. 7(a).
Γ_∞	1.88(2)		100–300 K, present α, C_p from Ref. 15
Γ_∞	1.8		200–300 K, Ref. 31
Γ_{lin}	4.5(5)		Graphical, Fig. 7(b)
$\Gamma_{spinglass}$	6.0(10)		Graphical, Fig. 7(b).

Γ_{ApQ} (—) in Fig. 7(b) can be used together with C_{pApQ} and Eq. (7) to calculate the smooth α_{ApQ} that is shown as the solid lines (—) in Figs. 4(a)–5(a), with the extrapolation from 17 to 0 K giving an approximate $\alpha_Q(T)$ for the non-spin-glass state. Between 17 and 108 K, α_{ApQ} reproduces α_Q with a standard deviation of 2%, is 5% larger at 27 K, and 3% smaller at both higher and lower temperatures.

The large spin-glass contribution to the thermodynamics of the quasicrystal makes it impossible to obtain directly from the present data a realistic estimate of the electronic contribution to C_{pQ}. Mizutani,[5] in a discussion of the role of the pseudogap in the electron transport of quasicrystals and their approximants, gives in his Fig. 4(a) the relationship between γ and the 300 K electrical resistivity (ρ) for these materials,

$$\ln(\rho/\mu\Omega\text{ cm}) = 2[1 - \ln(\gamma/\text{mJ/mol K}^2)]. \tag{8}$$

The anisotropic room-temperature resistivities for the approximant [Figs. 2(b)] and this relation give γ's [0.57 ($\perp$), 0.73 ($\parallel$) mJ/mol K^2] that are somewhat less than the experimental value (0.794 mJ/mol K^2) but which are within the scatter of his correlation. If the assumption is made that *i*-Al-Pd-Mn also is a member of this family, $\rho_Q = 1570$ $\mu\Omega$ cm at room temperature corresponds to $\gamma_Q = 0.25$ mJ/mol K^2. This is consistent with our earlier statement that the data plotted in Figs. 6 probably would reflect the existence of a γ only if its magnitude were greater than 0.4 mJ/mol K^2. Previously, extrapolations of high-temperature C_p data to $T = 0$ gave $\gamma_Q = 0.40(12)$ (Ref. 11) and ≈ 0.25 (Ref. 14) mJ/mol K^2. We cannot estimate the magnitude or sign of the corresponding linear term in the expansivity.

IV. SUMMARY

The initial objectives of these experiments were twofold. The first was to obtain high sensitivity low-temperature linear thermal expansivity (α) data for a quasicrystal, and, the second, to estimate ''normal'' lattice (non-spin-glass) thermodynamic properties for *i*-Al-Pd-Mn. Because of the range of stoichiometries reported for for these materials, C_p data also were obtained for the expansivity samples. Figures 3–5 give $\alpha(T)$ and $C_p(T)$ for a large single-grain sample of *i*-$Al_{71}Pd_{21}Mn_{08}$ (α_Q, C_{pQ}), as well as those for a similar sample of its $Al_{72}Pd_{25}Mn_{03}$ ξ' approximant (α_{Ap}, C_{pAp}). In Figs. 4 and 5, the behaviors of α_{Ap} and C_{pAp} are ''normal'' [Eqs. (3)], with $\gamma_{Ap} = 0.749(1)$ mJ/mol K^2 and $\Theta_{0Ap} = 455(3)$ K. As expected from magnetic measurements (Fig. 1), the approximant shows no magnetic contributions. The relatively large value of γ_{Ap} (compared with copper[39]) and the large electrical resistivities (Figs. 2) suggest the existence of a pseudogap that is characteristic of quasicrystals and re-

lated materials.[5] For the quasicrystal, α_Q and C_{pQ} clearly show the effects of the spin-glass transition[11,14] below 11 K, a temperature that is somewhat higher than has been proposed previously,[11,14] but, as with other *i*-Al-Pd-Mn properties, could be dependent on sample stoichiometry.

The relative 0 to 300 K length changes calculated from α_Q are consistent with those from x ray lattice parameter data.[30,31] The present α_{Ap} are for a single sample oriented parallel to the [010] axis. Figures 2 show that the resistivity of the approximant is anisotropic, and it is highly probable that α_{Ap} also will be anisotropic. The α_{Ap} and Γ_{Ap} results that are presented here are for this sample orientation only, and the analysis is highly oversimplified.[57]

The solid lines in Figs. 3–5 represent normalizations of the approximant data to those of the quasicrystal for $T>16$ K (α_{ApQ} and C_{pApQ}), which extrapolate the non-spin-glass α_Q and C_{pQ} to $T=0$. $C_{pApQ}(T)$ follows from the reduced equivalent Θ plot of Fig. 6(b), where the experimental $\Theta_{0Ap}=455$ K and $\Theta_{0ApQ}=480(1)$ K give a good correspondence between the quasicrystal and approximant C_p's for $T/\Theta_0>0.036$ (16 K). The C_{pAp}^{lat} relations [Eq. (5)] then, with $T_{ApQ}=T\times(455/480)$, generate C_{pApQ}.

$\Theta_{0Q}^{el}=505(1)$ K for the same material from RUS sound velocities [Eqs. (2)], vs 480 K from the normalization, and the systematic deviations in Fig. 6(b) between 0.02 and 0.03, suggest that the normalization breaks down slightly at low temperatures, and that the extrapolation of C_{pApQ} below 0.036 (16 K) will overestimate C_{pQ}^{lat} ($\Theta_{ApQ}<\Theta_Q$). A comparison with other ultrasonic elastic constant determinations of Θ_{0Q} (Table I) indicates a dependence on quasicrystal stoichiometry, with, qualitatively, $\Theta_{0Q}=504(10)$ K.

No direct means exist for determining the magnitude of an electronic contribution ($\gamma_Q T$) to C_{pQ}. If γ_Q were comparable in magnitude with γ_{Ap}, $\Theta_Q(T)$ would resemble $\Theta_{Aptot}(T)$ (●) in Figs. 6; since $\Theta_Q(T)$ behaves "normally" down to 11 K, the value $\gamma_Q\approx 0.25$ mJ/mol K^2, which follows from the 300 K resistivity-γ correlation proposed by Mitzutani[5] is reasonable. This would give a slight increase in C_{pApQ}/T in Figs. 4(b) and 5(b). Again, it is probable that spin glass[40] and electronic, as well as lattice, contributions to the quasicrystal thermodynamics depend on the stoichiometry. While the (extrapolated) lattice contribution to C_pQ is of the order of 10% at 3 K [Fig. 5(b)], its relative importance decreases rapidly at lower temperatures.

Figure 6(b) shows that Θ_{Ap}/Θ_{0Ap} decreases more rapidly with increasing temperature (shows greater dispersion, a more rapid deviation from the Debye function) than aluminum metal (a typical cubic metal), GaAs (a typical tetrahedrally bonded solid) or zinc metal (a typical anisotropic metal). This conclusion depends on the validity of Eq. (3b) to represent the C_{pAp} data and for the extrapolation to $T=0$. While the lack of a suitable sample prevented an RUS determination of the approximant sound velocities (Θ_{0Ap}^{el}), the relative agreement between the ultrasonic and normalized values of Θ_{0Q} suggests that $\Theta_{0Ap}=455(3)$ K is not seriously in error. A similar Θ_Q/Θ_{0Q} vs T/Θ_{0Q} relationship is expected for the quasicrystal, since $\Theta_Q(T)$ in Fig. 6(a) shows "normal" behavior down to 11 K ($T/\Theta_0=0.02$), where $\Theta_Q=355$ K and must increase to over 500 K at 0 K.

Wälti *et al.*[17] have suggested from an extrapolation of 18 to 8 K C_p data to lower temperature[11] [Fig. 4(b)] and from neutron-scattering results[19,21] that C_{pQ}^{lat} below 10 K is significantly greater than the one that would be calculated from the sound velocities and that this excess is nonacoustic in origin. The large dispersion effects displayed by the present data (which presumably are a property of the quasicrystal lattice) are consistent with and offer an explanation for their observations, with the experimental $C_{pQ}^{lat}\approx 45$ mJ/mol K at 10 K, to be compared with 15.5 mJ/mol K from the Debye model. The origin of this large dispersion is not clear, however, since inelastic neutron scattering data[21] are consistent with measured sound velocities and show dispersion only at energies (>1.5 THz), which are much larger than would be consistent with the present C_p results ($T<10$ K, or <0.2 THz). The generalized vibrational density of states (GVDOS)(Ref. 19) that follows from a thermal neutron energy loss scattering experiment assumes a Debye DOS (no dispersion) for an extrapolation from 8 meV (2 THz, 100 K) to 0; the extrapolation was not adjusted to agree with sound velocities in the low-energy limit. The present large dispersion effects unfortunately exist at energies that are inaccessible to the INS and GVDOS neutron-scattering investigations. Comparable C_p data for *i*-Al-Cu-Fe (Ref. 58) show dispersion similar to that for *i*-AlPdMn and its ξ' approximant, which suggests that this may be a common quasicrystal property. The existence of a low-lying optic mode probably is ruled out by the consistent values of γ and Θ_0 from fits of Eq. (3b) to the C_{pAp} data (see the discussion in Sec. III D).

INS data are taken mainly in the vicinity of strong Bragg reflections and along paths in reciprocal space towards another strong reflection for either the twofold or fivefold axes;[20] it is these results that show agreement with the ultrasonic data to relatively high energies (2 THz, 100 K) before nonlinear dispersion effects occur. The shapes of the higher-energy transverse acoustic dispersion relations depend significantly on the direction from the Bragg point in which the data are taken.[20] A possible resolution for the inconsistency between the C_p and neutron-scattering results is that the great number of phonons that are associated with much weaker Bragg reflections and directions away from the twofold and fivefold axes will show nonlinear dispersion relations at much lower energies than those reported in Ref. 20, and will be responsible for the large dispersion in C_p. Goldman *et al.*,[59] in an INS study of phonons in *i*- and *R*-phase (crystalline) Al-Cu-Li, discuss whether or not phonons exist off-major symmetry directions in icosahedral solids, and find slight differences between the quasicrystal and closely related crystalline materials. Quilichini and Janssen[60] in a summary of theoretical results for phonons in quasicrystals imply that very little is known about very low-energy phonon excitations in quasicrystals in low symmetry directions.

The temperature dependence of the (lattice) Grüneisen parameters [Eq. (7)] in Figs. 7 reflects the relationship between α_{Ap} and α_Q. The shapes and magnitudes of $\Gamma^{lat}(T)$ in Fig. 7(a) are normal for both solids, with Γ^{lat} approximately independent of temperature above 0.08 (40 K); this behavior

for Γ_Q continues to 300 K when the Cp's of Inaba *et al.*[15] are used (Table II). In Fig. 7(b), Γ_Q has a (spin-glass related) maximum near 0.01, while Γ_{Ap}^{lat} continues to increase with decreasing temperature to an (extrapolated) 0 K value ($\Gamma_{0Ap}^{lat}=11.3$) that is unexpectedly large. Above 13 K (0.027), Γ_Q and Γ_{Ap}^{lat} have very similar shapes, and $\Gamma_{ApQ}=0.948\Gamma_{Ap}^{lat}$ (—) reproduces the Γ_Q data very well. Γ_Q is systematically larger than Γ_{ApQ} between 0.027 and 0.012, so the extrapolation to 0 K using Γ_{ApQ} probably underestimates the actual $\Gamma_Q^{lat}(T)$. The increase with decreasing temperature of both Γ_Q and Γ_{Ap} below 30 K (0.06) reflects significantly different temperature dependences for α and for C_p. This is apparent in Figs. 5, especially for the quasicrystal, where C_{pAp}/T shows ''normal'' behavior (upward curvature, T^5 term >0), while α_{Ap}/T has a downward curvature (T^5 term <0). These shape differences persist beyond 20 K for both materials, and result in the increases of $\Gamma(T)$ with decreasing temperature and the (extrapolated) large value of Γ_{0Ap}^{lat}.

The lowest-temperature Γ_Q's in Fig. 7(b) (<0.01 or 5 K) correspond to those for the spin glass, with $\Gamma_{spinglass}=6(1)$. The source of the excess scatter in α_Q (Γ_Q) is not known. The relation $\Gamma_{ApQ}=0.948\,\Gamma_{Ap}^{lat}$ and the smooth C_{pApQ} were used with Eq. (7) to extrapolate $\alpha_Q^{lat}(T)$ below 13 K (—) in Figs. 4 and 5.

Equations (2) and (7) relate Γ_0^{lat} to the volume (pressure) dependence of the sound velocities (elastic constants) that have been reported by Amazit *et al.*[18,24] Unfortunately, their results show frequency and nonlinear pressure dependences that most likely are associated with relaxation effects.[24] Their high-pressure asymptotic results are consistent with $\Gamma_{0Ap}^{lat}\approx 2$, which is appreciably smaller than we observe (>10). Their measurements were taken along major symmetry directions, however, and to resolve the dispersion inconsistencies between calorimetric and neutron data we have postulated quite different properties for off-major symmetry direction phonons.

Another possibility is that our large Γ_{0Ap}^{lat} is associated with the tunneling that has been observed in other studies.[13,25,33] Tunneling should, however, be reflected in the Γ which is associated with the linear terms in α_{Ap} and C_{pAp}, and which is a relatively ''normal'' $\Gamma_{lin}=4.1(5)$. Tunnelling could make a relatively small (linear in T) contribution to C_p, which, with a very large Γ, could have a proportionally large effect on α. There is, unfortunately, no way of sorting out the existence of such a third contribution, which, at low temperatures, would be small for C_p but relatively large for α. The increase in Γ with decreasing temperature is continuous and smooth, beginning near 30 K, and it is difficult to foresee the tunneling effects at these relatively high temperatures.

V. CONCLUSIONS

Figures 6 and 7 summarize the present data for *i*-Al-Pd-Mn and its ξ' approximant. The major conclusion is that the lattice properties of both materials show very strong dispersion effects; that is, for C_p, deviations from the Debye model occur at an unusually low temperature (below 1 K), while the Grüneisen parameters, which reflect the volume dependence of lattice frequencies, also show an unusual temperature dependence and, for the approximant, large magnitudes below 6 K. The onset of the transition to a spin-glass state ($T_f<1.8$ K) dominates the quasicrystal, not the approximant, thermodynamics below 11 K, but a close similarity between the quasicrystal and the approximant data above 16 K allows an extrapolation of the quasicrystal data to lower temperatures to approximate the non-spin-glass state. Neutron-scattering results show that dispersion effects should occur only at relatively high energies (and temperatures), quite the opposite from the conclusion from our C_p data. The answer may lie in the behavior of very low energy, off-major symmetry, quasicrystal ''phonons'' that cannot be studied with current neutron-scattering techniques. Although the RUS measurements (Sec. III C) show that elastic waves are propagated in all directions in the quasicrystal, a legitimate question is to ask whether or not phonons, as defined for crystalline media, also exist for all directions in a quasicrystal.

ACKNOWLEDGMENTS

The authors wish to express their appreciation to Professor J. C. Lasjaunias for considerable correspondence and suggestions, and to Professor Alan Goldman for suggesting the potential importance of very low energy phonons to explain the C_p-neutron-scattering inconsistencies. We would like to thank M. J. Foley and N. D. Kelso for help in sample preparation and V. Fournée for compositional analysis of the Al-Pd-Mn ξ' approximant. This manuscript has been authored by Iowa State University of Science and Technology under Contract No. W-7405-ENG-82 with the U.S. Department of Energy.

*Email address: swenson@ameslab.gov

†Present address: Department of Applied Physics, Stanford University, Stanford, CA 94305

[1] D. Schectman, I. Blech, D. Gratia, and J.W. Cahn, Phys. Rev. Lett. **53**, 1951 (1984).

[2] A. P. Tsai, in *Physical Properties of Quasicrystals*, edited by Z. M. Stadnik (Springer, New York, 1999).

[3] I.R. Fisher, M. Kramer, Z. Islam, T.A. Wiener, A. Kracher, A.R. Ross, T.A. Lograsso, A.I. Goldman, and P.C. Canfield, Mater. Sci. Eng., A **294-296**, 10 (2000).

[4] G.A.M. Reynolds, G. Golding, A.R. Kortan, and J.M. Parsey, Phys. Rev. B **41**, 1194 (1990).

[5] U. Mizutani, J. Phys.: Condens. Matter **10**, 4069 (1998).

[6] E. Belin-Ferré, in *Quasicrystals*, edited by J.-M. Dubois, P.A. Thiel, A.-P. Jsai, and K. Urbar, MRS Symposia Proceedings No. 553 (Materials Research Society, Pittsburgh, 1999), p. 347.

[7] Z.M. Stadnik, D. Purdie, M. Garnier, Y. Baer, A.P. Tsai, A. Inoue, K. Edagawa, S. Takeuchi, and K.H.J. Buschow, Phys. Rev. B **55**,

10 938 (1997).
[8] R. Escudero, J.C. Lasjaunias, Y. Calvayrac, and M. Boudard, J. Phys.: Condens. Matter **11**, 383 (1999).
[9] T. Schaub, J. Delahaye, C. Berger, T. Grenet, H. Guyot, R. Belkhou, A. Taleb-Ibrahimi, J.J. Préjean, and Y. Calvayrac, Mater. Sci. Eng., A **294-296**, 512 (2000).
[10] E.S. Zijlstra and T. Janssen, Europhys. Lett. **52**, 578 (2000).
[11] M.A. Chernikov, A. Bernasconi, C. Beeli, A. Schilling, and H.R. Ott, Phys. Rev. B **48**, 3058 (1993).
[12] M.A. Chernikov, A. Bernasconi, C. Beeli, and H.R. Ott, Europhys. Lett. **21**, 767 (1993).
[13] M.A. Chernikov, A. Bianchi, and H.R. Ott, Phys. Rev. B **51**, 153 (1995).
[14] J.C. Lasjaunias, A. Sulpice, N. Keller, J.J. Préjean, and M. de Boissieu, Phys. Rev. B **52**, 886 (1995).
[15] A. Inaba, A.-P. Tsai, and K. Shibata, in *Proceedings of the 6th International Conference on Quasicrystals, Avignon, France*, edited by S. Takeuchi and T. Fujiwara (World Scientific, Singapore, 1998), p. 443.
[16] M.A. Chernikov, E. Felder, A.D. Bianchi, C. Wälti, M. Kenzelmann, H.R. Ott, K. Edagawa, M. de Boissieu, C. Janot, M. Feuerbacher, N. Tamura, and K. Urban, in *Proceedings of the 6th International Conference on Quasicrystals, Avignon, France* (Ref. 15), p. 451.
[17] C. Wälti, E. Felder, M.A. Chernikov, H.R. Ott, M. de Boissieu, and C. Janot, Phys. Rev. B **57**, 10 504 (1998).
[18] Y. Amazit, M. Fischer, B. Perrin, A. Zarembowitch, and M. de Boissieu, Europhys. Lett. **25**, 441 (1994).
[19] J.-B. Suck, J. Non-Cryst. Solids **153-154**, 573 (1993).
[20] M. de Boissieu, M. Boudard, R. Bellissent, M. Quilichini, B. Hennion, R. Currat, A.I. Goldman, and C. Janot, J. Phys.: Condens. Matter **5**, 4945 (1993).
[21] M. Boudard, M. de Boissieu, S. Kycia, A.I. Goldman, B. Hennion, R. Bellissent, M. Quilichini, R. Currat, and C. Janot, J. Phys.: Condens. Matter **67**, 7299 (1995).
[22] R.A. Brand, M. Krisch, M. Chernikov, and H.R. Ott, Ferroelectrics **250**, 233 (2001).
[23] Y. Amazit, M. de Boissieu, and A. Zarembowitch, Europhys. Lett. **20**, 703 (1992).
[24] Y. Amazit, M. Fischer, B. Perrin, and A. Zarembowitch, in *Proceedings of the 5th International Conference on Quasicrystals, Avignon, France*, edited by C. Janot and R. Mosseri (World Scientific, Singapore, 1995), p. 584.
[25] N. Vernier, G. Bellessa, B. Perrin, A. Zarembowitch, and M. de Boissieu, Europhys. Lett. **22**, 187 (1993).
[26] T. Tanaka, Y. Mitarai, and M. Koiwa, Philos. Mag. A **73**, 1715 (1996).
[27] A. Migliori and J.L. Sarro, *Resonant Ultrasound Spectroscopy* (Wiley, New York, 1997).
[28] Y. Amazit, B. Perrin, M. Fischer, J.P. Itie, and A. Polian, Philos. Mag. A **75**, 1677 (1997).
[29] Y. Yokoyama, A. Inoue, and T. Masumoto, Mater. Trans., JIM **34**, 135 (1993).
[30] A. Kupsch and P. Paufler, Z. Kristallogr. **214**, 681 (1999).
[31] K. Kajiyama, K. Edagawa, T. Suziki, and S. Takeuchi, Philos. Mag. Lett. **80**, 49 (2000).
[32] I.R. Fisher, M.J. Kramer, T.A. Wiener, Z. Islam, A.R. Ross, T.A. Lograsso, A. Kracher, A.I. Goldman, and P.C. Canfield, Philos. Mag. B **79**, 1673 (1999).
[33] E. Thompson, P.D. Vu, and R.O. Pohl, Phys. Rev. B **62**, 11 437 (2000).
[34] W.A. Phillips, Rep. Prog. Phys. **50**, 1657 (1987).
[35] M. Audier, M. Durand-Charre, and M. de Boissieu, Philos. Mag. B **68**, 607 (1993).
[36] T. Gödecke and R. Luck, Z. Metallkd. **86**, 109 (1995).
[37] S. Matsuo, H. Nakano, T. Ishimasa, and M. Mori, J. Phys. Soc. Jpn. **62**, 4044 (1993).
[38] C.A. Swenson, in *Thermal Expansion of Solids*, edited by C.Y. Ho and R.E. Taylor, CINDAS Data Series on Material Properties Vol. I-4 (ASM, Materials Park, OH, 1998), Chap. 8.
[39] C.A. Swenson, Rev. Sci. Instrum. **70**, 2728 (1999).
[40] J.C. Lasjaunias (private communication).
[41] J.S. Dugdale, *The Electrical Properties of Disordered Metals* (Cambridge University Press, Cambridge, England, 1995).
[42] H. Akiyama, T. Hashimoto, T. Shibuya, K. Edagawa, and S. Takeuchi, J. Phys. Soc. Jpn. **62**, 639 (1993).
[43] L. Beraha, M. Duneau, H. Klein, and M. Audier, Philos. Mag. A **76**, 587 (1997); V. Fournee, A.R. Ross, T.A. Lograsso, J.W. Anderegg, C. Dong, M.J. Kramer, I.R. Fisher, P.C. Canfield, and P.A. Thiel (unpublished).
[44] S. Martin, A.F. Hebard, A.R. Kortan, and A.R. Thiel, Phys. Rev. Lett. **67**, 719 (1991).
[45] I.R. Fisher, M.J. Kramer, Z. Islam, A.R. Ross, A. Kracher, T.A. Wiener, M.J. Sailer, A.I. Goldman, and P.C. Canfield, Philos. Mag. B **79**, 425 (1999).
[46] P.S. Spoor, J.D. Maynard, and A.R. Kortan, Phys. Rev. Lett. **75**, 3462 (1995).
[47] B_S/B_T and C_p/C_v are given by $C_p/C_v = B_S/B_T = [1 + \beta^2 B_S V/C_p T] = [1 + \beta\Gamma T]$, where $\beta = 3\alpha$ and Γ is the Grüneisen parameter, which will be described in Sec. III D. This ratio is 1.004 at 108 K (and negligible; no distinction will be made between C_p and C_v when discussing the present data), but is significant (1.022) at 300 K.
[48] T.H.K. Barron, J.G. Collins, and G.K. White, Adv. Phys. **29**, 609 (1980).
[49] T.H.K. Barron, in *Thermal Expansion of Solids* (Ref. 38), Chap. 1.
[50] E.S.R. Gopal, *Specific Heats at Low Temperatures* (Plenum, New York, 1966).
[51] T.H.K. Barron and J.A. Morrison, Can. J. Phys. **35**, 799 (1957).
[52] J.C. Holste, Phys. Rev. B **6**, 2495 (1972), with supplementary material in NAPS Document No. 01893; from ASIS/NAPS, c/o Microfiche Publications, 248 West Hempstead Turnpike, West Hempstead, NY 11552.
[53] C.A. Swenson, J. Phys. Chem. Solids **29**, 1337 (1968).
[54] See EPAPS Document No. E-PRBMDO65-039218 for the parameters for the fits of the various power series to the α and C_p data, together with encapsulated PostScript files for the figures appearing in this paper. This document may be retrieved via the EPAPS homepage (http://www.aip.org/pubservs/epaps.html) or from ftp.aip.org in the directory /epaps/. See the EPAPS homepage for more information.
[55] R. Stedman, L. Almqvist, and G. Nilsson, Phys. Rev. **162**, 549 (1967).
[56] W.T. Berg, Phys. Rev. **167**, 583 (1968), with C_p results from 2.7 to 20 K which show that Θ increases anomalously from $\Theta_0 = 428$ K to 438 K near 14 K, then decreases in agreement with Ref. 55.
[57] C.A. Swenson, Phys. Rev. B **53**, 3669 (1996), where α and C_p

data comparable with the present are discussed for anisotropic (hexagonal) crystals.

[58] C.A. Swenson and T.A. Lograsso (unpublished), α and C_p data for *i*-Al-Cu-Fe.

[59] A.I. Goldman, C. Stassis, M. de Boissieu, R. Currat, C. Janot, R. Bellissent, H. Moudden, and F.W. Gayle, Phys. Rev. B **45**, 10 280 (1992).

[60] M. Quilichini and T. Janssen, Rev. Mod. Phys. **69**, 277 (1997).